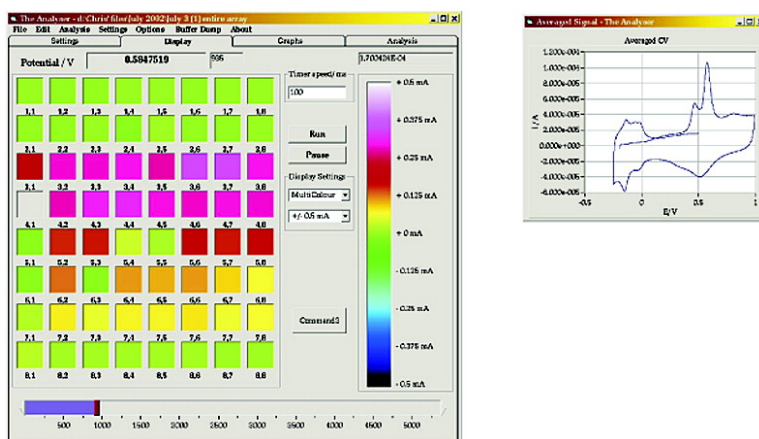


Combinatorial Electrochemical Screening of Fuel Cell Electrocatalysts

Samuel Guerin, Brian E. Hayden, Christopher E. Lee, Claire Mormiche,
 John R. Owen, Andrea E. Russell, Brian Theobald, and David Thompsett

J. Comb. Chem., **2004**, 6 (1), 149-158 • DOI: 10.1021/cc030113p • Publication Date (Web): 09 December 2003

Downloaded from <http://pubs.acs.org> on March 20, 2009



More About This Article

Additional resources and features associated with this article are available within the HTML version:

- Supporting Information
- Links to the 3 articles that cite this article, as of the time of this article download
- Access to high resolution figures
- Links to articles and content related to this article
- Copyright permission to reproduce figures and/or text from this article

[View the Full Text HTML](#)

Combinatorial Electrochemical Screening of Fuel Cell Electrocatalysts

Samuel Guerin, Brian E. Hayden,* Christopher E. Lee, Claire Mormiche,
John R. Owen, and Andrea E. Russell

*Combinatorial Chemistry Centre of Excellence, Department of Chemistry, University of Southampton,
SO17 1BJ, United Kingdom*

Brian Theobald and David Thompsett

*Johnson Matthey Technology Centre, Blount's Court,
Sonning Common, Reading, RG4 9NH, United Kingdom*

Received June 24, 2003

Combinatorial methods have been applied to the preparation and screening of fuel cell electrocatalysts. Hardware and software have been developed for fast sequential measurements of cyclic voltammetric and steady-state currents in 64-element half-cell arrays. The arrays were designed for the screening of high-surface-area supported electrocatalysts. Analysis software developed allowed the semiautomated processing of the large quantities of data, applying filters that defined figures of merit relevant to fuel cell catalyst activity and tolerance. Results are presented on the screening of carbon-supported platinum catalysts of varying platinum metal loading on carbon (and thus, particle size) in order to demonstrate the speed and sensitivity of the screening methodology. CO electro-oxidation, oxygen reduction, and methanol oxidation on a series of such catalysts reveal clear trends in characteristics and activities. Catalysts with smaller particle sizes reveal structure in the CO stripping voltammetry that can be associated with edge sites in addition to the closely packed planes, and this is concomitantly reduced as particle size is increased. Specific activity for steady-state methanol oxidation and oxygen reduction at room temperature in H₂SO₄ electrolyte is found to be a maximum for the largest particle sizes, in agreement with the literature. These trends in activity are significantly smaller than the differences in activities of promoted platinum-based alloy catalysts for the same reaction.

Introduction

Combinatorial screening is a newly emerging methodology for the rapid screening of electrocatalysts, particularly as those for use as anode or cathode catalysts of low-temperature polymer electrolyte membrane fuel cells (PEMFC). The simultaneous synthesis and screening of a large number of potentially active catalysts under identical conditions relevant to the PEMFC environment is clearly an attractive prospect in the search for new active and robust materials. The application of combinatorial screening methodologies to the study of electrocatalysts poses several problems in that a truly parallel cyclic voltammetric screening method requires the simultaneous potentiostatic control and measurement of current at a large number of electrodes. Such a multiplexing function is not readily available using commercially available instrumentation. Several research groups have reported alternate methods to efficiently obtain this multiplexing advantage of a parallel screen or have developed serial methods to characterize libraries of electrode reactions or electrocatalysts.

Perhaps the first report of combinatorial electrochemical screening was that of Reddington and co-workers.¹ Their method was based on an optical response of a fluorescent dye to changes in the local pH brought about by the electrochemical reaction of interest. In their first report, the

method was applied to the screening of catalysts for methanol oxidation.¹ Subsequently, the method has been applied to the discovery of electrocatalysts for oxygen reduction and water oxidation^{2,3} and catalysts for amperometric glucose sensors.⁴ The method has the advantage of the simplicity of a single working electrode and that electrochemical control and measurement are maintained using a single potentiostat and current follower. The principal limitation of the method is the relative insensitivity (signal-to-noise) of the optical response when compared to the measurement of electrode current directly. In addition, the use of a proton-sensitive dye in the electrolyte limits the range of experimental conditions (e.g., pH), and there is the added possibility that the dye may adsorb or react at the electrode surface and so influence the activity of the catalyst undergoing screening.

The use of an array of independently addressable catalyst electrodes, rather than a single electrode on which an array of catalysts is deposited, enables the direct current measurement at each electrode and obviates the requirement of an indicator. Such arrays of electrodes may be screened rapidly in series either using moveable counter and working electrodes that are brought into electrochemical contact with each of the individual working electrodes in turn^{5,6} or using a single electrochemical cell containing all of the working electrodes in the same electrolyte solution and fixed counter and reference electrodes.^{7,8} The moveable electrode method

* Corresponding author.

has been applied to the screening of a 144-element array of commercial electrocatalyst powders in Nafion for methanol oxidation⁵ and to the screening of photoelectrochemical materials.⁶ This approach, although economical, requiring only one potentiostat and current follower, is inherently slow as a result of the need to move the counter and reference electrodes. The serial examination of each electrode in the array or library in the same electrochemical cell using one potentiostat and current follower has been applied to the study of organosulfur monolayers adsorbed on gold electrodes.^{7,8} The principal disadvantage of such an approach, other than speed, is that the nonactive working electrodes remain in contact with the solution and reactants at open circuit while the active working electrode is screened.

Improved multiplexing in the screening of electrochemical libraries has been reported by Hintsche et al.⁹ They developed special ASIC switches that enabled the application of a potential to all the working electrodes of the library via bias lines, whereas the currents from individual working electrodes were read in series. Such a pseudoparallel method is more economical than very large multipotentiostats while retaining much of the multiplexing advantage of such systems.

We have adopted a similar approach, allowing a pseudoparallel screening of electrode materials deposited on independently addressable electrodes in a common electrolyte. Combining the use of a single channel potentiostat and a multi-channel current follower, fast sequential monitoring of the electrode currents is achieved. The rate of data collection is limited only by the speed of the data acquisition card and the computer. As such, this method may be envisaged as a pseudoparallel experiment. Since the electrochemical processes at the electrodes are occurring simultaneously (the potential at each electrode is the same), it is only the data collection process that is serialized. This approach has recently also been applied to the screening of positive electrode candidates for lithium batteries.¹⁰ The Hudson group has used a similar system of electrochemical instrumentation based on commercially available components from Scriber, Inc. These authors studied the spatial pattern forming at corroding electrodes using a multielectrode array.^{11,12} Results are presented for the combination of a single-channel potentiostat in conjunction with a 64-channel current follower, the latter interfaced to a PC via a commercially available multichannel A/D converter. A cell consisting of a 64-element array of electrodes for the screening of supported high-surface area electrocatalysts has also been constructed.

To demonstrate the sensitivity, reproducibility, and speed of the combined experimental system, we present results obtained for the oxidation of adsorbed carbon monoxide and methanol in solution and the reduction of oxygen on a series of carbon-supported platinum catalysts of varying particle sizes.

Experimental Section

All experiments were conducted using a purposely built computer-controlled electrochemical screening apparatus. A standard three-electrode potentiostat was used in conjunction with a programmable triangular wave generator and a 64-

channel current follower. Acquisition and control of the electrochemical system was achieved using a PCI-DAS6402/16 data acquisition card (Talisman Electronic) and a Pentium 4 (2.2 GHz) desktop computer operating under the Windows XP operating system. The data acquisition card incorporated 64 × 16 bits A/D inputs, 2 × 16 bits D/A outputs, and 4 TTL digital outputs. Figure 1 is a schematic representation of the electrochemical control system. A combination of D/A and digital outputs was used to program the limits of the triangular sweep. The potential was applied to the potentiostat and simultaneously monitored on one of the 64 channels of the data acquisition card. The remaining 63 channels were connected to 63 current followers at a fixed range of 1 mA/V. The range of the current follower and the maximum current of the potentiostat (3 A) were chosen to provide an optimized measurement system for this investigation. (We have also constructed current followers with 100 and 10 μ A/V ranges. These were used in conjunction with more sensitive potentiostats (1- and 2-A maximum currents) for the electrochemical characterization of 100-element, thin film electrode arrays (to be published). Current followers with all these ranges are available within the research group, and when combined with a choice of potentiostats with maximum current of either 1, 2, or 3 A, provide an optimized measurement system for each investigation.

Two Visual Basic software applications were written, one mainly to acquire, and the second to analyze, the data. Both programs allow the user to either monitor one electrode at a time, displaying the cyclic voltammogram, the current transient, or the charge transient, or allow the response of all 63 electrodes to be observed simultaneously using false color response. The acquisition is done sequentially; a value is collected from each channel before starting to collect a second value. Furthermore, an averaged value for each channel is produced for every 100 values per channel. The user may adjust the number of data points averaged per channel. The data acquisition card can achieve 200 kHz total sampling rate, thus giving a maximum speed per channel of 3125 Hz if using 64 channels simultaneously. Typically, the sampling rate per channel was set at 1 kHz and the average per channel done over 100 points per channel. This gives an apparent sampling rate of 10 Hz per channel. The averaging was necessary in order to achieve the desired level of signal to noise. Therefore, a set of the resulting 63 electrode data is generated, plotted, and saved in 0.10 s. This corresponds to, for example, a complete 1.2-V range voltammogram of each working electrode at a typical sweep rate of 50 mV/s completed simultaneously in 48 s. The second program served to automate the data analysis. In particular, we were able to integrate chosen regions of the voltammograms, pick out peak potentials, and measure peak currents as single operations for each of the electrodes on the array.

The 8 × 8 array and electrochemical cell for the screening of high-surface-area supported electrocatalyst samples is shown in Figure 2. A similar version of this cell has recently been used for the screening of battery electrode materials.¹⁰ Sixty-four glassy carbon rod electrodes (3-mm diameter) were embedded in a glass-filled PTFE block, with an inter-electrode spacing of 9 mm. The electrochemical cell was

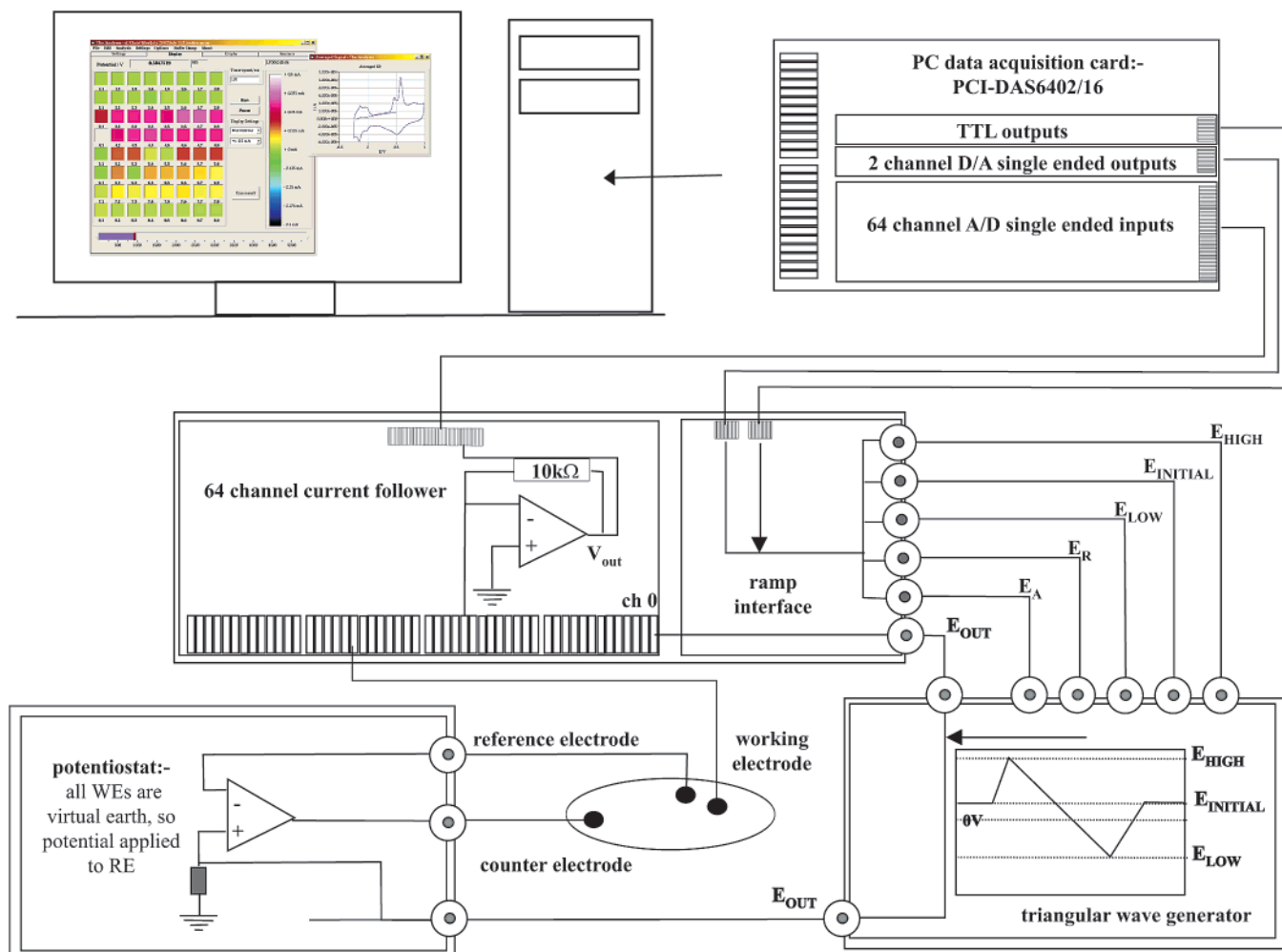


Figure 1. Schematic of the modular electrochemical control system developed for the combinatorial electrochemical screening experiments. There are several modules depicted above. Among them are the computer for data acquisition (top), a 64-channel current follower (center), a potentiostat (bottom left), a triangular sweep generator (bottom right), and an electrochemical array cell (bottom center).

constructed from Teflon, and the cell was sealed onto a glass filled PTFE block using a KALREZ O-ring. The cell top was a piece of glass cut to fit with several holes in it to allow gases to be delivered into the cell and also to support the reference electrode. Electrical connections to the glassy carbon rods were achieved using spring-loaded pins which were soldered onto a printed circuit board located underneath the cell.

All electrolyte solutions used, unless otherwise stated, were 0.5 M $\text{H}_2\text{SO}_4(\text{aq})$ which was prepared from concentrated H_2SO_4 (Aldrich, 99.999% purity) and ultrapure water (Millipore). Carbon monoxide (BOC, CP grade 99%) and nitrogen (BOC, oxygen-free OFN) were used for adsorption of carbon monoxide on the catalysts and for purging the electrolytes. A series of eight Pt/C catalysts with platinum loadings ranging from 10 to 78 wt % Pt supported on Vulcan XC-72 carbon was supplied by Johnson Matthey and prepared as previously reported.¹³ The fuel cell grade Pt black (an unsupported material consisting of nanoscale Pt particles) used was also obtained from Johnson Matthey. All electrochemistry experiments were performed under a $\text{N}_2(\text{g})$ atmosphere in deaerated electrolytes unless noted otherwise. Methanol (Aldrich, ACS spectrophotometric grade 99.9%)

was used as received. Experiments using the 64-electrode array were all conducted using a commercial saturated calomel reference electrode (SCE, Cole Parmer, +0.241 V vs SHE), but potentials reported here are given relative to the hydrogen electrode (SHE).

The vitreous carbon electrodes were cleaned with detergent, ultrapure water, ethanol; then polished with 1- μm Al_2O_3 power and ultrapure water; and finally, rinsed with ethanol then ultrapure water prior to application of the electrocatalyst deposits.

Electrocatalyst deposits were prepared from volumetric suspensions of Pt/C powders containing Nafion in glacial acetic acid. The amount of Nafion in the deposits was controlled by the addition of 50 μL of 5 wt % Nafion suspension to the glacial acetic acid and Pt/C mixtures prior to diluting the suspensions to the 1.00-mL mark. To ensure homogeneous suspensions, the contents of the volumetric flasks were vigorously shaken and agitated using an ultrasound bath for several hours prior to use. During the transfer of aliquots of the electrocatalyst suspensions, the volumetric flasks were immersed in the operating ultrasound bath throughout the procedure. Prior to commencing the electrochemical screening experiments, the deposits required a brief conditioning period. During conditioning, the potential was cycled be-

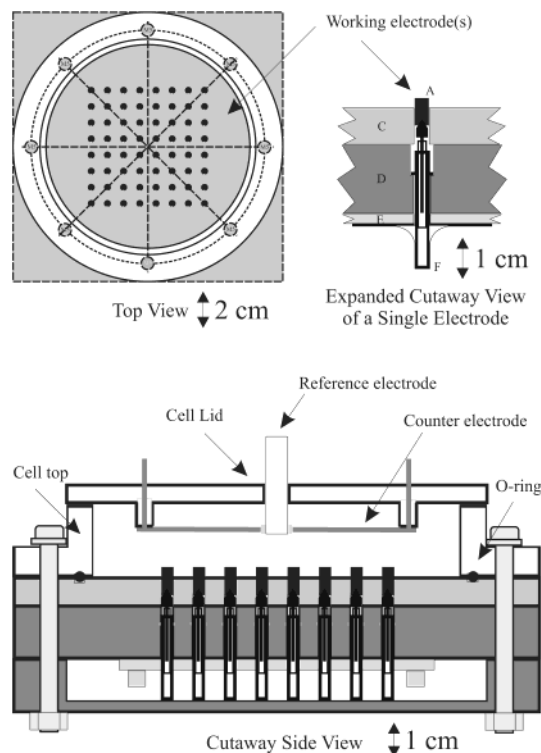


Figure 2. Schematic of the cell (viewed from the top, the side, and an expanded view of a single electrode) used for electrochemical screening of the 64-element array: vitreous carbon electrode (A), spring-loaded electrical contact, glass filled PTFE array base plate (C), polypropylene contact holder (D), and a printed circuit board (E).

tween 0.025 and 1.2 V vs SHE for up to 1 h at 20 mV/s. This procedure was required to remove any disadvantageous adsorbates from the catalyst deposits and to ensure that the Nafion-bound catalyst layers were fully hydrated.

Carbon monoxide stripping voltammetry was carried out on the electrocatalyst deposits with saturation coverages of CO produced by exposure to a CO saturated solution under potential control at 75 mV vs SHE for 30 min. Subsequently, any CO remaining in the bulk electrolyte was removed by purging with N₂ for 30 min prior to completing the stripping voltammetry. To perform potentiostatic methanol oxidation experiments, the electrodes were held at 75 mV vs SHE for 5 min while sufficient methanol was added to prepare a 1.0 M solution. The electrolyte was mixed by bubbling with N₂(g) during this time. The potential was then stepped from 75 mV to 0.6 V, and the current time transients were recorded for 5 min. Oxygen reduction experiments were performed as follows. The electrodes were held at 1.2 V vs SHE for 5 min while the electrolyte was saturated with oxygen. The potential was subsequently stepped in 100 to 25 mV increments from 1.2 to 0.5 V vs SHE at 90-s intervals, and the steady-state currents were recorded.

Results and Discussion

Vitreous (glassy) carbon supporting electrodes were used in the high surface area sample array, since the electrochemical response of the polished electrodes is well-defined, and the currents associated with them are small. Figure 3 includes

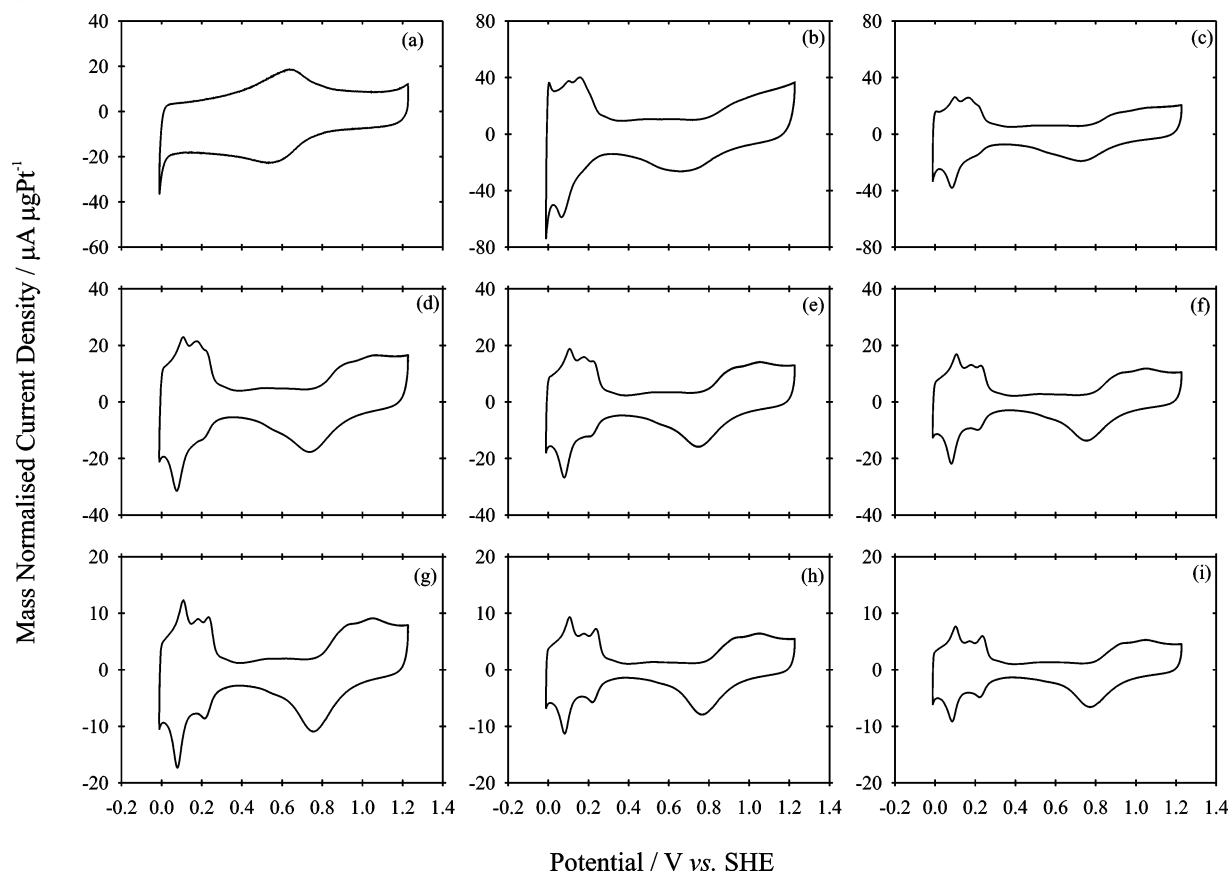


Figure 3. Typical voltammograms of (a) a vitreous carbon supporting electrode and of a series of Pt/C electrocatalyst deposits (b) 10, (c) 20, (d) 30, (e) 40, (f) 50, (g) 60, (h) 70, and (i) 78 wt % Pt recorded at 20 mV/s in 0.5 M H₂SO₄(aq). With the exception of the voltammogram of the vitreous carbon electrode (a) in which the unit of the ordinate is micromaperes, the currents for the Pt/C catalysts are normalized to the mass of Pt.

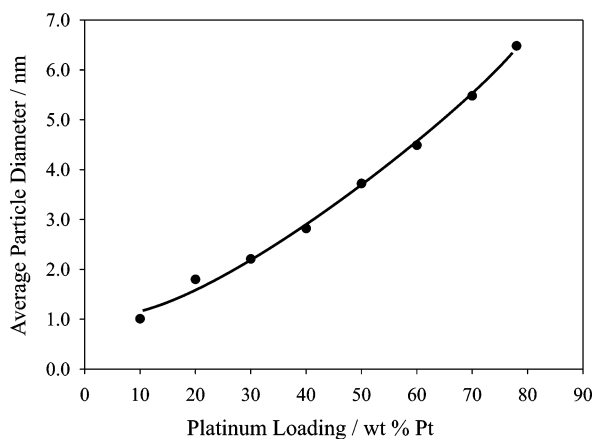


Figure 4. Average particle diameters measured by XRD vs the Pt loadings.

(a) the voltammogram of one of the glassy carbon electrodes of the array. Note that the ordinate is expressed in microamperes and not in microamperes per microgram of platinum for this pane of the figure only. The reversible peak in the carbon voltammogram is due to the interconversion of quinone and hydroxyquinone surface groups.¹⁴ Figure 3 also shows the voltammetry of a selection from a 64-element array series of platinum catalysts supported on carbon (Vulcan XC-72R) with eight different platinum loadings ranging from 10 to 78%, obtained in 0.5 M H₂SO₄(aq) at 20 mV/s. The array was organized in groups of four identical deposits and two deposit loadings of 20 and 40 μ g of the Pt/C catalyst for each of the platinum loadings. It is important to note that platinum loading refers to the amount of Pt per unit mass of Pt/C catalyst, and it is expressed as a weight percent, whereas the deposit loading refers to the actual amount of Pt/C catalyst on an electrode, and it is expressed in micrograms. This arrangement provided sufficient replicate data for statistical analysis while allowing variation in deposit loadings that would indicate any experimental artifacts that may be attributed mass transport limitations during oxygen reduction and methanol oxidation. The hydrogen underpotential deposition (UPD) features, measured as a function of platinum loading, exhibited changes concomitant with the increasing particle size. As anticipated, the currents for the 20- μ g loading electrodes were one-half those of the 40- μ g loadings, verifying that no electrode thickness effects were present.

The average particle sizes of the series of Pt/C electrocatalysts were measured by X-ray diffraction (XRD). The results are summarized in Figure 4. The average particle diameters ranged from 1 to 6.5 nm for the 10–78 wt % Pt/C catalysts, respectively. The real surface areas are the surface areas of the catalysts on the electrode measured directly from the cyclic voltammetry. These depend on the mass of the catalyst deposited on the electrode. The real surface areas were extracted using a standard literature method from the cathodic hydrogen UPD and are plotted in Figure 5.¹⁵ The real surface areas of the catalysts obtained by this method ranged from 3 to 16 cm². The mass of Pt on each electrode ranged from 2.5 to 35 μ g, depending on the platinum loading of the catalyst. The specific surface area of a supported catalyst is the amount of available catalyst surface per unit

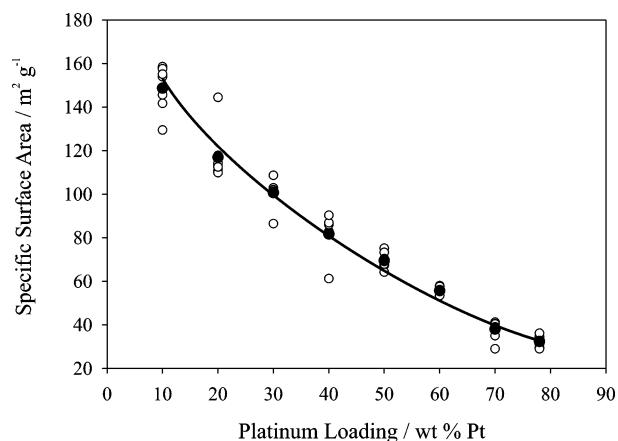


Figure 5. Specific surface areas measured by electrochemical means vs the Pt loadings. The open circles are all of the available data, and the closed circles are average values.

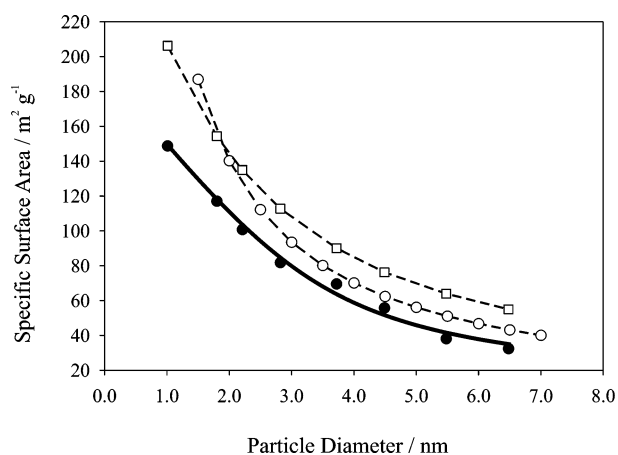


Figure 6. The average specific surface areas vs the average particle diameters for a series of Pt/C electrocatalysts. The closed circles are the experimental data, the open circles are calculated values assuming spherical particles, and the open squares are calculated values assuming cubooctahedral particles.

of mass of the catalyst, usually expressed in square meters per gram. The corresponding specific surface areas of the platinum component of these catalysts ranged from 30 m² g⁻¹ for the 78 wt % Pt/C to 150 m² g⁻¹ for the 10 wt % Pt/C. It is well-known that increasing the platinum loading during that catalyst synthesis results in the formation of larger-diameter particles. The relationship between the electrochemically measured specific surface areas and the average particle diameters is shown in Figure 6. Also shown in Figure 6 is an estimate of surface area as a function of particle size. The size of the supported crystallites was estimated from the widths of the Pt X-ray diffraction peaks,¹⁶ and the corresponding surface areas were calculated assuming that the particles were spherical particles (open circles) or half cubooctahedral, assuming the basal plane of the particle is occluded.¹⁷ It is apparent that the measured surface areas are slightly lower than the values estimated from the X-ray data, indicating that the metal particles do not exhibit their maximum theoretical dispersion. This is not unexpected, since the metal particles are not ideal spheres and are not monodispersed. In addition, it is likely that some of the metal surface area is occluded by the carbon support. The specific current densities, microamperes per square centimeter,

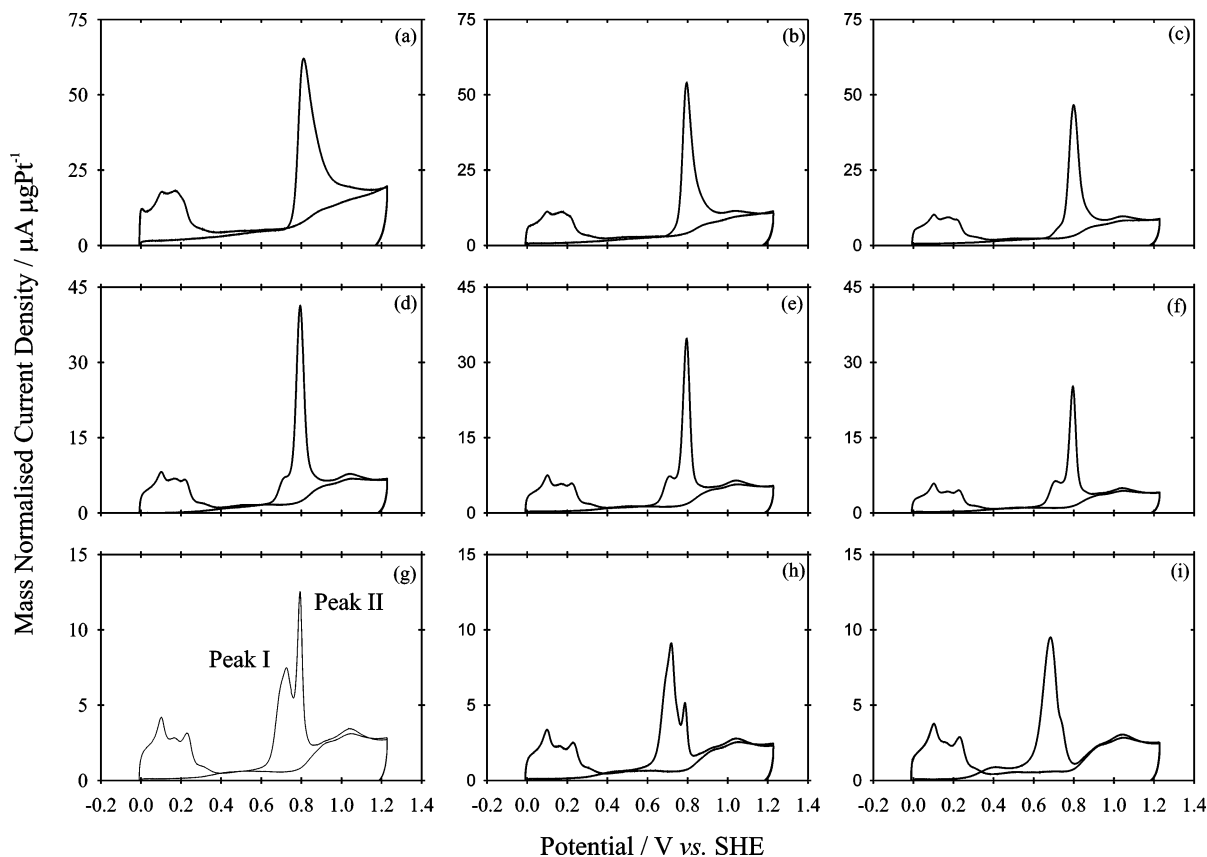


Figure 7. Typical carbon monoxide stripping voltammograms for a series of Pt/C electrocatalyst deposits (a) 10, (b) 20, (c) 30, (d) 40, (e) 50, (f) 60, (g) 70, (h) 78 wt % Pt and of (i) Pt black recorded at 10 mV/s in 0.5 M H₂SO₄(aq). The currents are normalized to the mass of Pt.

reported below were calculated by normalizing the measured currents to the electrochemical surface areas determined from the cathodic hydrogen region.

The measurement of the electrochemical behavior of these catalysts in the H₂SO₄ supporting electrolyte alone was a prelude to a series of measurements relevant to their activity of catalysts in anode and cathode reactions of the low-temperature PEMFC and DMFC (direct methanol fuel cell). This series of pure platinum catalysts of varying particle sizes were not chosen because they represent potentially state-of-the-art active catalysts for all of the reactions studied. Rather, they were chosen because distinguishing differences between these catalysts is a sensitive measurement of the methodology for active catalyst screening. The expected differences as a function of particle size are much smaller than differences induced by, for example, alloying platinum with a second metal component, a common methodology for increasing the activity and tolerance of electrocatalysts. For example, the activity of Pt has previously been found to increase by a factor of 30 by alloying it with 10 at. % Ru.¹⁸ The differences anticipated between the activities of the pure platinum catalysts are significantly lower. In addition, Pt/C catalysts are known to be stable under the electrochemical conditions to which they were subjected in these studies. We were thus able to separate problems related to the instrumentation and experimental methods from those that arise as a result of unstable catalyst compositions.

The series of catalysts were screened for their activity toward the electro-oxidation of methanol, the oxidative stripping of carbon monoxide, and the reduction of oxygen. Particle size effects are known to exist for all of these reactions.^{19–21} Carbon monoxide stripping has been used to estimate the real surface areas of Pt based electrocatalysts,²² but more importantly, carbon monoxide oxidation has been used as a measure of potential CO tolerance for PEM anode catalysts²² and often correlates with the activity of platinum-based catalysts in methanol electro-oxidation under conditions in which CO poisoning, and hence its removal, is rate limiting.²³

Figure 7 shows typical carbon monoxide stripping voltammograms for each of the series of the (10–78 wt %) Pt/C and for a Pt black catalyst. All of the voltammograms show complete poisoning of hydrogen adsorption by adsorbed CO, confirming that saturation of the Pt surface with CO was complete in each case. Note also that the width, position and number of CO stripping peaks vary as a function of platinum loading. A single peak is observed for the 10 and 20 wt % Pt deposits (see panes a and b). As the platinum loading is increased, a peak at lower over-potential begins to increase in intensity at the expense of the higher potential peak. When the platinum loading is increased beyond 70 wt %, as in pane h, the lower potential peak becomes the major peak. The peak potentials for the lower and upper potential peaks were 0.69 and 0.79 V. The positions of these peaks remained constant as the catalyst loading was varied;

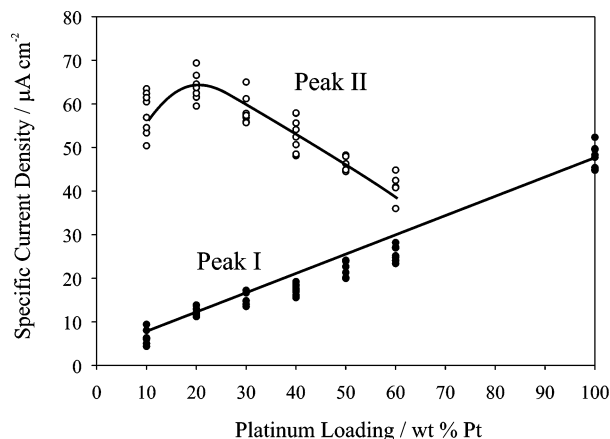


Figure 8. Current densities for peak I (closed circles) and peak II (open circles) vs Pt loading observed during the carbon monoxide stripping experiments.

however, the relative intensities (peak current) were found to depend on the catalyst loading and, therefore, particle size. The Pt black deposit, pane i, appears to exhibit the lowest over-potential for the electro-oxidation of adsorbed carbon monoxide, and the higher potential peak appears only as a shoulder on the anodic side of the main peak. A particle size effect for the electro-oxidation of adsorbed CO has also been observed by Takusa et al. in $\text{HClO}_4(\text{aq})$, although these authors adsorbed carbon monoxide in the double layer region and observed only a single peak with a potential that decreased as particle size increased.²¹

Figure 8 shows the effects of increasing platinum loading (and thus, particle diameter) on the specific current densities of the carbon monoxide stripping peaks. There is an increase in the specific current density of the lower potential peak (peak I) at the expense of that of the higher potential peak (peak II) as the particle size increases. As summarized by Kinoshita in his discussion of particle size effects for oxygen reduction, there is a significant decrease in the number of edge and corner sites as the fraction of terrace sites increases

with particle size.¹⁹ A possible interpretation of the CO stripping voltammetry is, therefore, that peak I is a result of the oxidation of CO(ads) on the terraces and that peak II is a result of the oxidation of CO(ads) on or near edge and corner sites. The ease with which the larger particles eliminate adsorbed carbon monoxide parallels their increases in specific activity toward the electro-oxidation of methanol as particle size increases (vide infra). It has been suggested that the particle size effect for the electro-oxidation of methanol (and other small molecules whose oxidation proceeds via CO(ads)) is a result of an increase in the proportion of terrace sites as the particle diameter increases.²⁰ It has also been reported that the binding energy of CO and also of OH increases as Pt particle size decreases.²⁴ The lower reactivity of strongly adsorbed CO is argued to be the reason for its more extensive poisoning at edge sites and could also be associated with the higher effective over-potential observed in the CO stripping voltammetry. However, we cannot exclude the possibility that different facets are responsible for the observed trends in CO stripping, as argued for methanol and oxygen reduction (below). According to Attard et al. the features of the hydrogen UPD region may be used to characterize the surface crystallography of Pt particles.²⁵ The absence of a clear interpretation of the hydrogen adsorption/desorption peaks in the hydrogen UPD region (for which there are also apparent trends with particle size) prevents us from making a more definitive statement concerning the origin of the observed trends for CO oxidation (Figure 8).

Figure 9 shows the specific current densities and also the mass normalized current densities at each of the catalysts of the Pt/C series, as well as their average values (filled circles), for the electro-oxidation of methanol at 0.6 V. These currents were measured 1 min after stepping the potential to 0.6 V. All of the data shown in the plot were generated in a single experiment. That is, each data point (open circles) was obtained for an individual catalyst deposit on a different

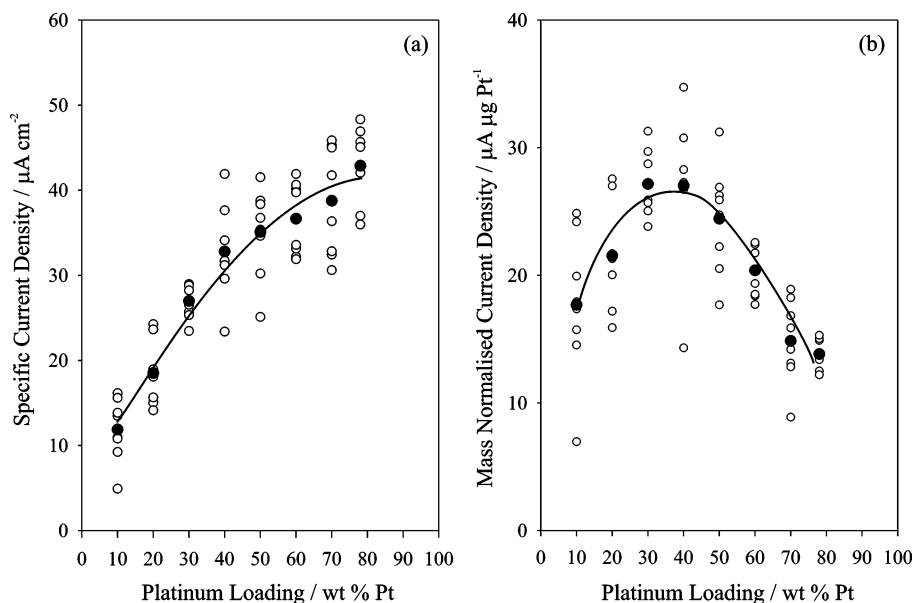


Figure 9. Current densities (a) per unit of surface area and (b) per unit mass of Pt for the electro-oxidation of methanol at 0.6 V vs SHE in 1.0 M $\text{CH}_3\text{OH}(\text{aq})$, 0.5 M $\text{H}_2\text{SO}_4(\text{aq})$ for the Pt/C catalysts plotted as a function of Pt loading. The open circles are all of the available data, and the closed circles are average values.

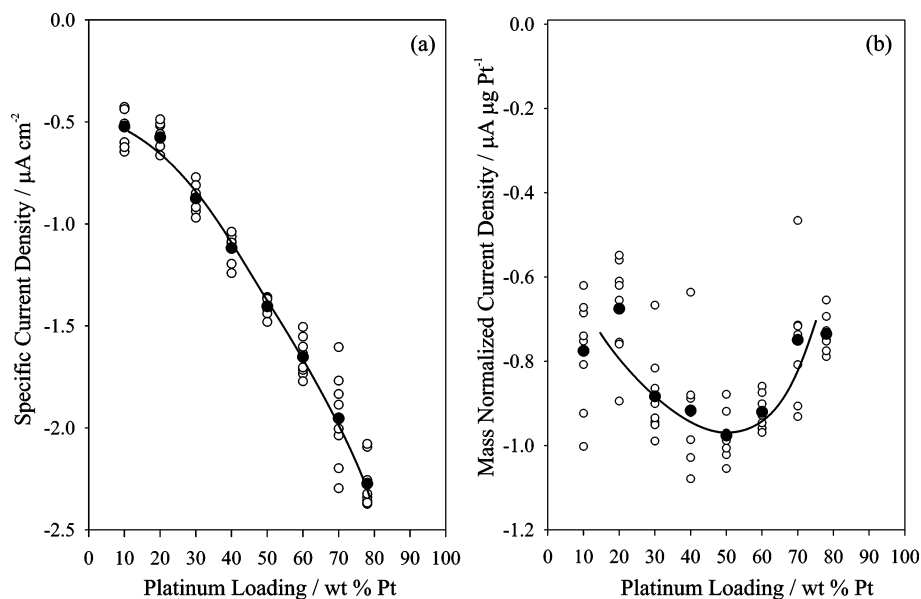


Figure 10. Current densities (a) per unit of surface area, and (b) per unit mass of Pt for the electroreduction of oxygen at 0.85 V vs SHE in oxygen saturated 0.5 M H₂SO₄(aq) for the Pt/C catalysts plotted as a function of Pt loading. The open circles are all of the available data, and the closed circles are average values.

vitreous carbon electrode of the same 64-working electrode array. The average specific current densities ranged from 11.87 (3.70) to 42.88 (4.51) $\mu\text{A cm}^{-2}$. The values in parentheses are the standard deviations. It is clear from the specific current densities measured as a function of Pt loading that the activity of these Pt particles increases as the particle size increases. There is an increase in turnover of almost a factor of 4 upon increasing the average particle size from 1 to 6.5 nm. A similar trend was observed when the potential was stepped to 0.55 V, although the currents were lower. This result is consistent with earlier observations concerning particle size effects in methanol oxidation on platinum electrocatalysts in acid electrolytes.^{20,21,26}

The plot of the mass current densities vs Pt loading provides not only a direct “economic indicator” of their relative activity, but also (as in the case for oxygen reduction, described below) provides a test of models relating particle morphology, surface structure, and catalytic activity.¹⁹ It is apparent that the maximum mass activity is obtained for the 30 or 40 wt % Pt/C. This corresponds to Pt particles with diameters between 2 and 3 nm.

The particle size effects on methanol and carbon monoxide oxidation that we observed in H₂SO₄ electrolytes are in agreement with results reported by Takusa et al. in HClO₄, indicating that the surface-sensitive specific adsorption of anions is not a determining factor.²¹ It has been suggested that the effect of particle size on methanol oxidation is either a result of an absence of platinum ensembles for methanol adsorption at small particle sizes²⁰ or an increase in the proportion of terrace sites that facilitate the oxidative removal of CO(ads).^{24,27,28} It is interesting to note that the maximum in the mass activity corresponds to particle sizes (2–3 nm) only slightly smaller than that corresponding to the maximum in mass activity (3.5 nm) observed for the oxygen reduction reaction (ORR) shown in Figure 10. The latter is ascribed (see below) to the dominant activity of the (100) facets in ORR, with contribution of the (111) facets effectively

poisoned by the specific adsorption of sulfate anions. A similar crystal face dependence in specific activity to that proposed for ORR, for which the trend observed was (110) > (100) > (111)^{29,30} has been suggested for methanol oxidation.³¹ However, it should be noted that the (111) surface has been suggested to be the most active when modified by the spontaneous deposition of Ru.³² The absence of significant sulfate adsorption during methanol oxidation on (111) facets may make the contribution of (111) facets more significant in methanol oxidation, resulting in an optimum mass activity of ~ 2.5 nm for particles exposing both (100) and (111) facets.¹⁹

The most common use for Pt electrocatalysts in fuel cells at present is as cathode catalysts for the reduction of oxygen. That there is a particle size effect on the electroreduction of oxygen is well-known.^{14,33,34} There are several explanations for the particle size effect on oxygen reduction, including the stronger adsorption of oxygenated intermediates on smaller Pt particles³⁵ and the specific adsorption of anions (e.g., SO₄²⁻) blocking surface sites that predominate on the surfaces of particles as a function of their diameter.³⁰ Markovic et al. concluded that the active surface geometry for oxygen reduction belongs to the (100) sites and that (111) sites, edges, and corners were inactive. They concluded that the reduction of oxygen is adversely affected by the specific adsorption of anions.^{29,30}

The electro-reduction of oxygen (ORR) was studied under steady-state conditions. Figure 10 shows the specific current densities and mass current densities for ORR for each of the catalysts in the Pt/C series as well as their average values measured at steady-state at 0.85 V. The average specific current densities ranged from -0.523 (0.090) to -2.270 (0.121) $\mu\text{A cm}^{-2}$. The values in parentheses are the standard deviations. The specific current densities increase with increasing particle size, and the plot of mass current densities shows a maximum at 50 wt % Pt. Similar increases in specific activity and the presence of a maximum in the mass

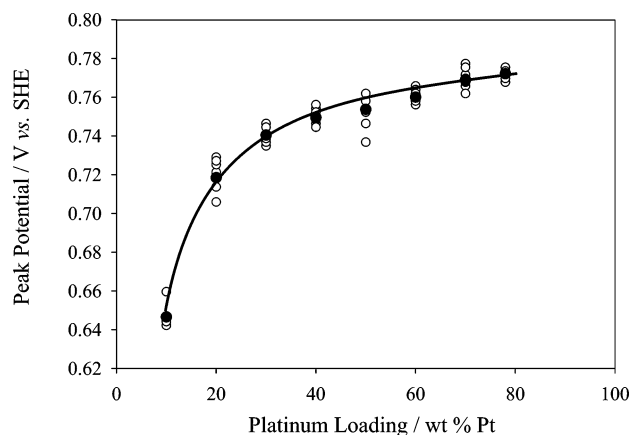


Figure 11. Peak potentials for the reduction of the Pt oxide as a function of Pt particle size. The data were obtained from voltammograms recorded at 20 mV/s in 0.5 M H₂SO₄(aq). The open circles are all of the available data, and the closed circles are average values.

activity for oxygen reduction as particle size increases have been previously reported.^{19,36} The observed maximum in the mass activity (Figure 10) corresponds to a particle size of 3.5 nm (Figure 5). Note that the currents are negative, and therefore, the maximum mass-normalized current density corresponds to a minimum in the curve shown in the diagram. The maximum activity for 3.5-nm particles is consistent with the predictions of Kinoshita, since this maximum in mass activity corresponds to the optimum in size for cubooctahedral particles to expose (100) facets.¹⁹ These results are therefore also in agreement with the experimental results of Markovic et al. that showed the (100) sites to be more active than (111)-oriented single crystals for the electroreduction of oxygen in sulfuric acid electrolytes because of the poisoning effect of specific adsorption of sulfate anions on Pt(111).²⁹

The ease of reduction of the platinum surface oxide is reflected in the oxide reduction potentials. These are plotted vs the electrocatalyst loadings in Figure 11. It is apparent from inspection of Figures 10 and 11 that the current densities for oxygen reduction are highest for the larger diameter particles and that the peak potential for the reduction of the surface oxide is also more anodic for the larger diameter particles. This relationship implies that the reduction of oxygen on platinum in H₂SO₄ is more facile on surfaces that do not strongly bind the oxide layer, a conclusion which has been made elsewhere.³⁵

Summary and Conclusions

Hardware and software have been developed for fast sequential measurements of cyclic voltammetric and steady-state currents in 64-element half-cell arrays. The arrays are designed for the screening of high surface area supported electrocatalysts. The analysis software developed enables the semiautomated processing of the large quantities of data. For example, filters may be applied which define figures of merit relevant to fuel cell catalyst activity and tolerance. That is, peak potentials, currents, and charges can be measured for all of the electrodes in a single step.

The high-surface-area catalyst screening array has been used to establish trends in CO electro-oxidation, oxygen

reduction, and methanol oxidation on a series of supported platinum catalysts as a function of platinum loading and, hence, particle size. The experimental methodology is sufficiently sensitive to reveal clear trends in characteristics and activities. Small particle sizes reveal structure in the CO stripping voltammetry that can be associated with edge sites in addition to the closely packed planes, and this is concomitantly reduced as particle size is increased. Specific activity for steady-state methanol oxidation and oxygen reduction at room temperature in H₂SO₄ electrolyte is found to be a maximum for the largest particle sizes, in agreement with the literature. The trends in activity reported are significantly smaller than the differences in activities of promoted platinum-based alloy catalysts for the same reactions. The experimental configuration is therefore shown to be highly effective for the screening of active supported catalysts for these and similar electrocatalytic reactions.

Acknowledgment. Funding for this work was provided by Johnson Matthey and by the Engineering and the Physical Sciences Research Council (EPSRC). The authors thank Tom Young for building the electrochemical instrumentation and also the mechanical workshop staff at the University of Southampton for the construction of the electrochemical array cell components.

References and Notes

- Reddington, E.; Sapienza, A.; Gurau, B.; Viswanathan, R.; Sarangapani, S.; Smotkin, E. S.; Mallouk, T. E. *Science* **1998**, *280*, 1735.
- Morris, N. D.; Mallouk, T. E. *J. Am. Chem. Soc.* **2002**, *124*, 11114.
- Chen, G. Y.; Delafuente, D. A.; Sarangapani, S.; Mallouk, T. E. *Catal. Today* **2001**, *67*, 341.
- Sun, Y. P.; Buck, H.; Mallouk, T. E. *Anal. Chem.* **2001**, *73*, 1599.
- Jiang, R.; Chu, D. *J. Electroanal. Chem.* **2002**, *527*, 137.
- Baek, S. H.; Jaramillo, T. F.; Brandli, C.; McFarland, E. W. *J. Comb. Chem.* **2002**, *4*, 563.
- Yudin, A. K.; Siu, T. *Curr. Opin. Chem. Biol.* **2001**, *5*, 269.
- Sullivan, M. G.; Utomo, H.; Fagan, P. J.; Ward, M. D. *Anal. Chem.* **1999**, *71*, 4369.
- Hintsche, R.; Albers, J.; Bernt, H.; Eder, A. E. *Electroanalysis* **2000**, *12*, 660.
- Spong, A. D.; Vitins, G.; Guerin, S.; Hayden, B. E.; Russell, A. E.; Owen, J. R. *J. Power Sources* **2003**, *119–121*, 778.
- Fei, Z.; Kelly, R. G.; Hudson, J. L. *J. Phys. Chem.* **1996**, *100*, 18986.
- Fei, Z.; Hudson, J. L. *J. Phys. Chem. B* **1997**, *101*, 10356.
- Keck, K.; Buchanan, H.; Hards, G. *Catalyst Material*; Johnson Matthey Public Limited Company: U.S.A., 1991.
- Kinoshita, K. *Carbon*; J. Wiley and Sons: New York, 1988; Chapter 6.
- Woods, R. *J. Electroanal. Chem.* **1974**, *49*, 217.
- Matyi, R. J.; Schwartz, L. H.; Butt, J. B. *Catal. Rev.-Sci. Eng.* **1987**, *29*, 41.
- Benfield, R. E. *J. Chem. Soc. Faraday Trans.* **1992**, *88*, 1107.
- Gasteiger, H. A.; Markovic, N.; Ross, P. N.; Cairns, E. J. *J. Phys. Chem.* **1993**, *97*, 12020.
- Kinoshita, K. *J. Electrochem. Soc.* **1990**, *137*, 845.
- Park, S.; Xie, Y.; Weaver, M. J. *Langmuir* **2002**, *18*, 5792.
- Takasu, Y.; Iwazaki, T.; Sugimoto, W.; Murakami, Y. *Electrochem. Commun.* **2002**, *2*, 671.

- (22) Schmidt, T. J.; Noeske, M.; Gasteiger, H. A.; Behm, R. J.; Britz, P.; Brijoux, W.; Bonnemann, H. *Langmuir* **1997**, *13*, 2591.
- (23) Gasteiger, H. A.; Markovic, N.; Ross, P. N.; Cairns, E. J. *Electrochim. Acta* **1994**, *39*, 1825.
- (24) Mukerjee, S.; McBreen, J. J. *Electroanal. Chem.* **1998**, *448*, 163.
- (25) Attard, G. A.; Gillies, J. E.; Harris, C. A.; Jenkins, D. J.; Johnston, P.; Price, M. A.; Watson, D. J.; Wells, P. B. *Appl. Catalysis A* **2001**, *222*, 393.
- (26) Kabbabi, A.; Gloaguen, F.; Andolfatto, F.; Durand, R. J. *Electroanal. Chem.* **1994**, *373*, 251.
- (27) Kabbabi, A.; Gloaguen, F.; Andolfatto, F.; Durand, R. J. *Electroanal. Chem.* **1994**, *373*, 251.
- (28) Frelink, T.; Visscher, W.; van Veen, J. A. R. *J. Electroanal. Chem.* **1995**, *382*, 65.
- (29) Markovic, N. M.; Gasteiger, H. A.; Ross, P. N. *J. Phys. Chem.* **1995**, *99*, 3411.
- (30) Markovic, N.; Gasteiger, H.; Ross, P. N. *J. Electrochem. Soc.* **1997**, *144*, 1591.
- (31) Clavilier, J.; Lamy, C.; Leger, J. M. *J. Electroanal. Chem.* **1981**, *125*, 249.
- (32) Tremiliosi-Filho, G.; Kim, H.; Chrzanowski, W.; Wieckowski, A.; Grzybowska, B.; Kulesza, P. *J. Electroanal. Chem.* **1999**, *467*, 143.
- (33) Bregoli, L. J. *Electrochim. Acta* **1978**, *23*, 489.
- (34) Thompsett, D. In *Handbook of Fuel Cells – Fundamentals, Technology and Applications*; Vielstich, W., Lamm, A., Gasteiger, H. A., Eds.; John Wiley & Sons: Chichester, 2003; Vol. 3, p 467.
- (35) Min, M. K.; Cho, J. H.; Cho, K. W.; Kim, H. *Electrochim. Acta* **2000**, *45*, 4211.
- (36) Antoine, O.; Bultel, Y.; Durand, R. *J. Electroanal. Chem.* **2001**, *499*, 85.

CC030113P